11-MeV Proton Optical-Model Analysis*

C. M. Perey, F. G. Perey, and J. K. Dickens
Oak Ridge National Laboratory, Oak Ridge, Tennessee 37830

AND

R. J. Silva
Oak Ridge Associated Universities, Oak Ridge, Tennessee 37830

(Received 10 July 1968)

An optical-model analysis of elastic scattering of 11-MeV protons from 24 nuclei in the mass range ^{45}Sc to ^{76}Ge is presented. The data analyzed include 18 angular distributions which we have measured and the previously published 10.5-MeV elastic-polarization data. An average set of geometrical parameters is determined for the data, and the real radius parameter of this potential is substantially larger than normally used at higher energies. The analysis performed with a fixed geometry, but allowing the well depths to be readjusted independently for each nucleus, reveals a very smooth dependence of the real-well depth as a function of mass number. However, the real-well depths fail to follow the expected isospin dependence of the optical potential.

I. INTRODUCTION

THE purpose of many proton optical-model analyses is to find an average potential which will fit as many sets of data as possible at different energies and to interpret the variations of the parameters in terms of nuclear properties of the target nuclei. Several recent analyses, in particular at 30 and 40 MeV,[1–3] using fairly complete sets of differential cross-section and polarization data, have shown results which differed significantly from earlier analyses[4,5] based on less complete neutron and proton data below 20 MeV. Since the 30- and 40-MeV data could not be analyzed on the basis of the lower-energy results, it is of considerable interest to see if the lower-energy data can be reproduced using a model determined from the 30- and 40-MeV analyses or if there is a definite change in the optical-model potential as a function of energy.

The description of elastic scattering by means of a one-body Schröedinger equation with a smooth local complex central potential plus a spin-orbit potential is a gross oversimplification of the problem. It is possible to write formal expressions for the optical-model potential[6,7] but so far it has been impossible to evaluate these expressions in a way that the results are directly applicable to the analysis of data. Because of the elimination of the nonelastic channels at least, the potentials are expected to have an energy dependence and at the lower energies this can be quite appreciable.[4] It is very difficult, with our present methods of optical-model studies, to determine precisely and unambiguously the optical-model potential parameters. It is well known that, using the conventional potential shapes, the analysis of scattering data from one nuclei at a given energy leads to nonunique parameters. This is probably so partially because we have standardized on inadequate shapes but also because in general the data does not define a unique scattering matrix. Even if it did it is quite possible for several distinct potentials to give, at one energy, essentially the same scattering matrix. However, the introduction of biases and constraints in the variation of the potential parameters when fitting several sets of data puts severe restrictions on the parameter space; it is usually thought that such average potentials are more meaningful.

The purpose of this paper is to report on a careful analysis of proton elastic scattering differential cross section and polarization data from medium weight nuclei at 11-MeV incident energy. The aim of this analysis was to find, at this energy, the best average potential for medium-weight nuclei; no attempt was made to insure that this potential would be adequate outside the range of nuclei considered and at other energies. This analysis differs significantly from previous ones in two important aspects: first, the large data set used covers a small mass range and second, the incident energy is the lowest at which such systematic analyses have been made.

The energy was selected for the following reasons: A complete set of polarization data was available;[8] some reaction cross sections in this energy region have been measured, and at 11 MeV, E_p is sufficiently above the (p,n) threshold for many medium-weight nuclei so that compound elastic scattering contributions were likely to be small. We have measured the differential scattering cross sections from 18 nuclei from ^{48}Ti to ^{76}Ge. From 12 of those data sets, we have determined an average set of geometrical parameters. With this average geometry we have analyzed data at 11 MeV from 25 nuclei in

* Research sponsored by the U. S. Atomic Energy Commission under contract with the Union Carbide Corp.

[1] G. W. Greenlees and G. J. Pyle, Phys. Rev. **149**, 836 (1966).
[2] M. P. Fricke and G. R. Satchler, Phys. Rev. **139**, B567 (1965); M. P. Fricke, E. E. Gross, B. J. Morton, and A. Zucker, *ibid.* **156**, 1209 (1967).
[3] G. R. Satchler, Nucl. Phys. **A92**, 273 (1967).
[4] F. G. Perey, Phys. Rev. **131**, 745 (1963).
[5] F. Bjorklund and S. Fernbach, Phys. Rev. **109**, 1295 (1958).
[6] H. Feshbach, Ann. Rev. Nucl. Sci. **8**, 49 (1958).
[7] R. Lipperheide, Nucl. Phys. **89**, 97 (1966).
[8] L. Rosen, J. G. Beery, A. S. Goldhaber, and E. H. Auerbach, Ann. Phys. (N. Y.) **34**, 96 (1965).

this mass range and studied the behavior of the dependence of the well depths as a function of nuclei.

II. CHOICE OF MODEL AND CRITERIA FOR ANALYSIS

The optical model used is defined by the sum of the following potentials:

1. Central potential,

$$\text{real part} \quad -V_s f(r,r_s,a_s),$$

$$\text{imaginary part} \quad 4a_D W_D \frac{d}{dr} f(r,r_D,a_D).$$

2. Spin-orbit potential,

$$\boldsymbol{\sigma}\cdot\mathbf{l}\left(\frac{h}{m_\pi c}\right)^2 \frac{V_{s0}}{r}\frac{d}{dr} f(r,r_{s0},a_{s0}).$$

3. Coulomb potential,

$$\begin{cases} (Ze^2/2R_c)(3-r^2/R_c^2) & \text{for } r\leq R_c, \\ Ze^2/r & \text{for } r>R_c. \end{cases}$$

The function $f(r,r_0,a)$ is the usual Fermi or Woods-Saxon form factor,

$$f(r,r_0,a)=\{1+\exp[(r-r_0A^{1/3})/a]\}^{-1},$$

where A is the atomic mass of the nucleus in atomic mass units.

The factor $4a_D$ in the imaginary potential is used so that the imaginary potential has a maximum value of W_D. The Coulomb potential written would be that produced by a uniform charge distribution of radius R_c. Since the results are not sensitive to the value of R_c, throughout this analysis it was kept fixed at $1.25A^{1/3}$ F. This model is the one most commonly used for optical-model analysis.[1-4]

The present analysis was made with an optical-model search code which minimizes χ^2 with respect to any number of parameters simultaneously. In order to convey an objective quantitative value of the quality of the fits, we shall define (in an obvious notation) the quantities χ_σ^2, χ_p^2, and $N\chi^2$ as follows:

$$\chi_\sigma^2=\frac{1}{N_\sigma}\sum_{i=1}^{N_\sigma}\left(\frac{\sigma_{\rm th}(\theta_i)-\sigma_{\rm expt}(\theta_i)}{\Delta\sigma_{\rm expt}(\theta_i)}\right)^2,$$

$$\chi_p^2=\frac{1}{N_p}\sum_{i=1}^{N_p}\left(\frac{P_{\rm th}(\theta_i)-P_{\rm expt}(\theta_i)}{\Delta P_{\rm expt}(\theta_i)}\right)^2,$$

$$N\chi^2=N_\sigma\chi_\sigma^2+N_p\chi_p^2.$$

The quality which the code minimizes is the total chi square $N\chi^2$. This is an arbitrary choice; e.g., one could have minimized the sum of χ_σ^2 and χ_p^2. Since, for our particular analysis, we are covering such a small range of A values, the curves are very similar and, regardless of the criteria used, the same weighting is applied to all distributions. If the analysis covered a larger range of masses at several energies, the two different criteria would not be equivalent.

III. DATA ANALYZED

A. Present Experimental Results

We shall consider separately two groups of differential cross-section data experimentally obtained at Oak Ridge.

1. For ^{48}Ti, ^{51}V, ^{52}Cr, ^{54}Fe, ^{56}Fe, ^{59}Co, ^{60}Ni, ^{62}Ni, ^{64}Ni, ^{63}Cu, ^{65}Cu, ^{64}Zn, ^{66}Zn, and ^{68} Zn all the targets were self-supporting foils of approximately 1.0 mg/cm^2. The isotopic enrichments were $\geq 95\%$ for all targets. The 11.0-MeV proton beam was obtained from the Oak Ridge National Laboratory (ORNL) Tandem Van de Graaff. Pulse-height spectra of the scattered charge particles were obtained at 5° intervals between laboratory angles of 20° and 165°. The detector was a solid-state surface-barrier counter, sufficiently deep to fully stop 11-MeV protons; the energy resolution was about 40 keV full width at half-maximum (FWHM). Details of the experimental procedure and data reduction are similar to those given elsewhere.[9] The numerical values of the cross sections of all the peaks for which we obtained angular distributions are available.[10] For elastic scattering the errors due to counting statistics were very small and from reproducibility studies we estimate the relative errors to be less than 5% for angles greater than 30°. Because of dead-time losses and inaccuracy in angle settings, the errors were larger at smaller angles. Angle settings were measured with a precision of 0.1° with respect to the geometrical zero line of the scattering chamber; the geometrical zero line was determined to be the beam line to within 0.3°. The absolute normalization assigned to the cross sections depended on the measured target thickness, the detector solid angle measurements, and the beam integration measurements. We estimate the accuracy of the absolute magnitude to be within 10%.

2. For the germanium isotopes we made measurements with self-supporting targets which were obtained from the evaporation of the germanium isotope onto Formvar backings. The targets were of considerably poorer quality resulting in less precise data, in particular, with respect to absolute magnitude. The data were analyzed because they extended the measurements to heavier masses but we shall not put much weight on the departure of the analysis from the trends when this occurs for the germanium isotopes.

[9] R. J. Silva and G. E. Gordon, Phys. Rev. **136**, B618 (1964).
[10] J. K. Dickens, F. G. Perey, and R. J. Silva, Oak Ridge National Laboratory Report No. ORNL-4182, 1967 (unpublished).

TABLE I. Optical-model parameters corresponding to the curves plotted on Figs. 1 and 2. All the parameters were adjusted by the code in order to obtain the minimum total χ^2's. The elastic cross-section data are normalized by the factors K.

Element	K	V_s (MeV)	r_s (F)	a_s (F)	W_D (MeV)	r_D (F)	a_D (F)	V_{s0} (MeV)	r_{s0} (F)	a_{s0} (F)	σ_R (mb)	χ_σ^2	χ_P^2	$N\chi^2$
^{48}Ti	1.00	52.88	1.255	0.390	20.91	0.968	0.333	8.76	0.976	0.280	693	1.7	3.4	106
^{51}V	1.00	50.05	1.240	0.666	8.37	1.270	0.620	7.87	1.303	0.619	959	0.78	2.5	61
^{52}Cr	1.00	48.85	1.260	0.658	11.07	1.285	0.461	9.63	1.278	0.482	841	0.77	2.1	59
^{54}Fe	1.00	45.61	1.306	0.701	19.37	1.370	0.293	8.68	1.284	0.359	787	0.93	1.1	48
^{56}Fe	1.00	45.34	1.322	0.652	12.87	1.297	0.484	7.79	1.323	0.517	944	1.7	3.0	94
^{59}Co	0.90	45.41	1.313	0.682	11.72	1.354	0.500	6.43	1.307	0.587	995	1.1	0.88	48
^{60}Ni	1.00	47.39	1.289	0.720	13.47	1.333	0.456	7.70	1.304	0.506	962	0.17	0.31	10
	1.05[a]	47.38	1.290	0.707	13.09	1.341	0.455	7.67	1.313	0.513	950	0.12	0.34	8.9
^{62}Ni	0.95	47.08	1.291	0.711	11.32	1.356	0.511	5.79	1.234	0.565	1023	0.40	0.67	22
^{64}Ni[b]	1.00	50.12	1.271	0.663	12.14	1.298	0.50[c]	6.31	1.285	0.50[c]	966	1.4	3.3	146
^{63}Cu	1.00	48.52	1.269	0.753	16.58	1.439	0.319	6.72	1.417	0.393	920	0.86	0.81	38
	0.95[a]	48.95	1.261	0.760	15.56	1.426	0.351	6.58	1.392	0.427	940	0.54	0.80	28
^{65}Cu	0.90	50.20	1.283	0.627	11.09	1.265	0.500	7.30	1.267	0.437	904	2.1	2.5	104
^{64}Zn	0.90	46.77	1.287	0.753	12.70	1.397	0.444	5.94	1.281	0.497	991	0.30	3.6	65
^{66}Zn	0.95	52.12	1.246	0.648	8.46	1.235	0.666	5.86	1.082	0.474	961	0.80	1.5	48
^{68}Zn	1.00	47.74	1.307	0.660	12.76	1.305	0.490	6.14	1.200	0.410	987	0.48	0.61	23

[a] Curves corresponding to these renormalized data not shown on Figs. 1 or 2.
[b] Nickel-62 and ^{64}Zn polarization data used.
[c] Value of parameter not adjusted by code.

As a matter of convenience in the search, we assigned to all these data an error of 7.5% for angles up to 30° and 5% at greater angles.

B. Cross-Section Data Previously Measured

All of the polarization data were taken by Rosen *et al.*[8] at an energy of 10.5 MeV. We have also included differential cross sections for 10.9-MeV protons elastically scattered from ^{58}Fe (Ref. 11) to which we assigned an error of 7.5%.

C. Organization of the Analysis

The first phase of the analysis, for a determination of a set of best-fit potentials, was done on the 14 nuclei for which we had both differential cross-section and polarization measurements (^{48}Ti,^{51}V,^{52}Cr,^{54,56}Fe,^{59}Co, ^{60,62,64}Ni,^{63,65}Cu,^{64,66,68}Zn). Since there were no polarization measurement for ^{64}Ni, a set combining the polarization data of ^{62}Ni and ^{64}Zn was used. Thus, there were 30 polarization "data" points for ^{64}Ni, instead of 15 as for the other nuclei, a point to bear in mind when comparing the total χ^2 for this isotope to the total χ^2 for the other nuclei.

The second phase of the analysis was the determination of an average set of geometrical parameters, and is described more fully in Sec. V. The best-fit parameters for the ^{48}Ti and ^{54}Fe data were considered too divergent from the values found for the other isotopes; therefore, the ^{48}Ti and ^{54}Fe data were excluded during the search for an average geometry.

The last stage of the analysis was the study of the trends of the optical-model potential-well depths, and is described more fully in Sec. VI. In addition to the 14 isotopes previously mentioned, the analysis included the following additional data:

1. Differential cross-section and polarization data: ^{58}Fe.
2. Differential cross-section data only: ^{70,72,74,76}Ge.
3. Polarization data only: ^{45}Sc, ^{49}Ti, ^{55}Mn, ^{57}Fe, and ^{58}Ni.

IV. BEST-FIT POTENTIALS

The automatic searches for best-fit potentials were started from the results of a previous analysis.[12] The following starting values were used for all isotopes:

$$V_s=50\text{ MeV},\quad r_s=1.25\text{ F},\quad a_s=.65\text{ F},$$
$$W_D=13\text{ MeV},\quad r_D=1.25\text{ F},\quad a_D=.47\text{ F},$$
$$V_{s0}=5.5\text{ MeV},\quad r_{s0}=1.17\text{ F},\quad a_{s0}=.47\text{ F}.$$

The automatic searches were conducted in four steps:

1. Three-parameter search: Only the three well depths were varied. The results can be summarized as follows:

$$49<V_s<53,\quad 6<W_D<14,\quad 6<V_{s0}<9.$$

2. Four-parameter search: The three well depths and the diffuseness parameter a_D were optimized.
3. Eight-parameter search: All of the parameters but r_{s0} were optimized.
4. All nine parameters were adjusted.

The final results are shown in Figs. 1 and 2 and the parameters are given in Table I. The quality of the fits is very satisfactory and in most cases the χ^2/point is about 1.

The gradual increase of the number of parameters being varied by the search code, in general, allows the code to converge in a controlled manner. For two of the

[11] J. Benveniste, A. C. Mitchell, and C. B. Fulmer, Phys. Rev. 133, B317 (1964).

[12] F. Perey, in *Proceedings of the Second International Symposium Polarization Phenomena of Nucleons Karlsruhe*, edited by P. Huber and H. Schopper (W. Rosch and Co., Bern, 1966), p. 191.

nuclei ^{59}Co and ^{64}Ni some difficulties were experienced when all the parameters were varied. Those difficulties were traced to the following causes:

1. ^{59}Co. The search fails to converge if all three parameters of the spin orbit potential are allowed to vary. Convergence could be achieved only if one of these parameters was left free.

2. ^{64}Ni. Divergence of the search occurred when both a_D and a_{s0} were allowed to vary. Values of $a_D = a_{s0} = 0.5$ F were found to be the most adequate.

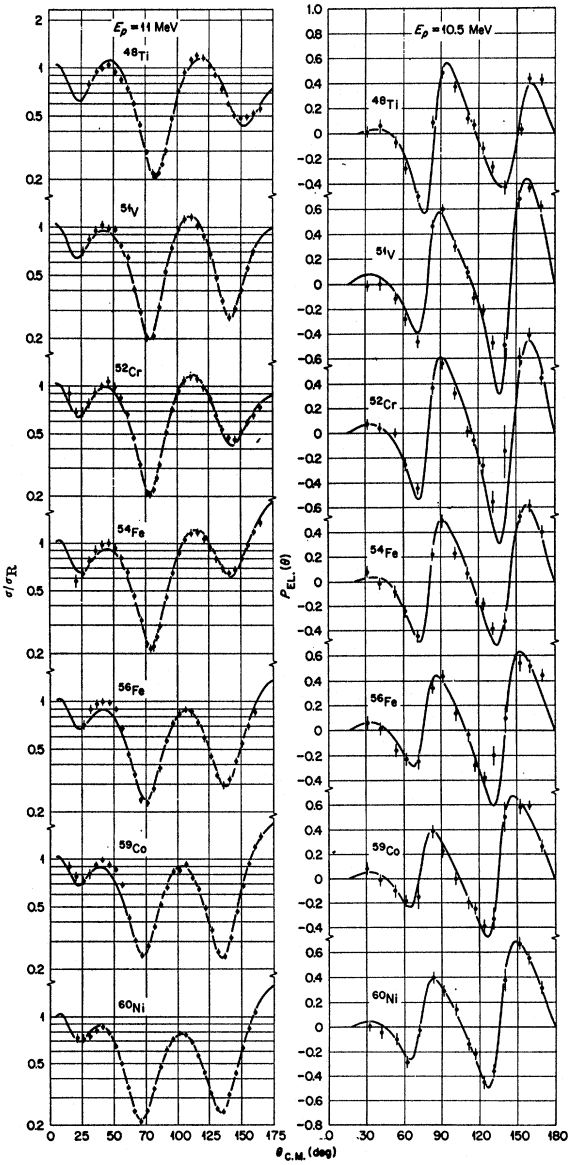

FIG. 1. Best fits to the 11-MeV elastic cross-section and 10.5-MeV elastic-polarization data. All the parameters of the model were adujsted by the code in order to obtain the minimum total χ^2 for each nucleus. The parameters corresponding to these curves are given in Table I.

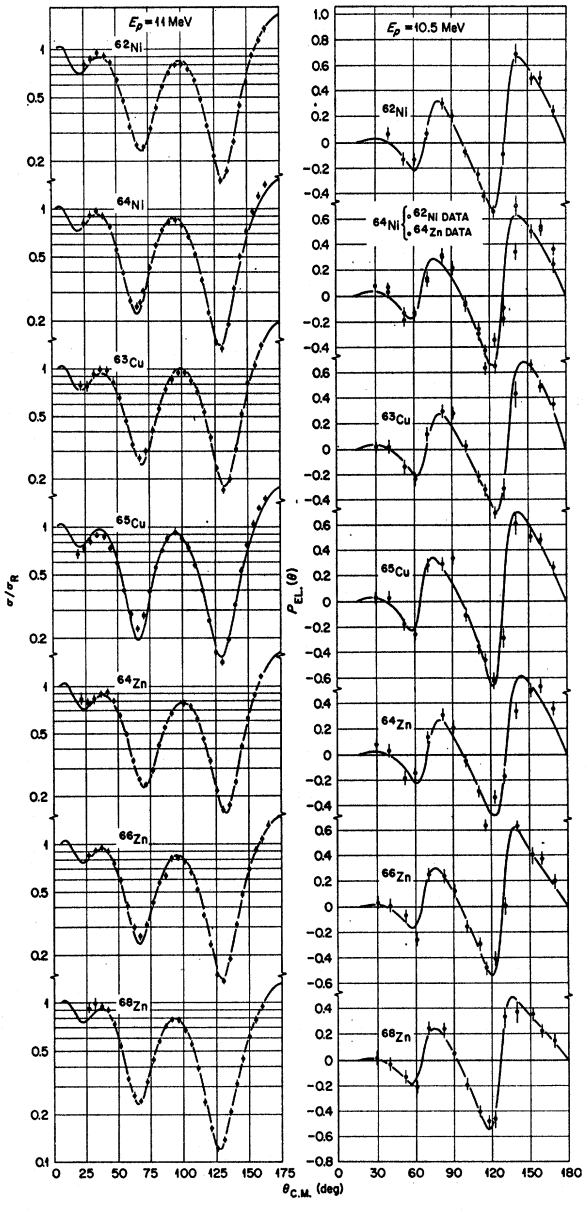

FIG. 2. Best fits to the 11-MeV elastic cross-section and 10.5-MeV elastic-polarization data. All the parameters of the model were adjusted by the code in order to obtain the mimimum total χ^2 for each nucleus. The parameters corresponding to these curves are given in Table I.

A. Renormalization

Since the absolute values of the cross sections were known experimentally to $\pm 10\%$ we investigated the effect of renormalization of the data on the optical-model potential searches. When the data showed systematic departures from the optical-model curves for angles less than 50° renormalization of the data in steps of 5% was studied. If, within the experimental errors on normalization, a new fit could be obtained which did not appreciably change the χ^2 for the polarization but

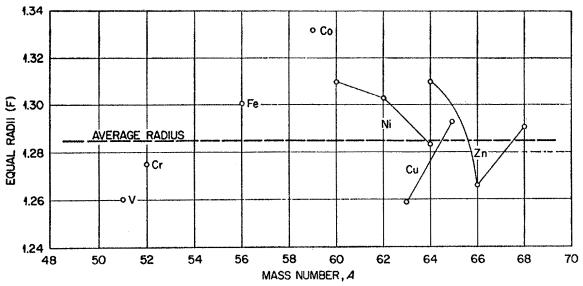

FIG. 3. Values of the radius parameter for each nucleus obtained from the search I_1. For each nucleus, the radius parameters of the three well depths were restricted to be equal and this value, along with the six other parameters of the optical-model potential, were adjusted by the code in order to obtain the minimum total χ^2's given in Table III, column I_1. The dashed line indicates the average value of the equal radius parameters, $r=1.285$ F, adopted for all the nuclei in the following searches.

improved the χ^2 for the differential cross section by 50% (the ratio of the χ^2 before normalization to the χ^2 after renormalization greater than 1.5), the renormalized data was accepted. New normalization of the data for four isotopes and the redetermined χ^2's are shown in Table II.

The renormalization by 10% of the data for ^{65}Cu was not based on the above criteria since the data at angles less than 50% were fitted in a satisfactory manner. We were prompted to investigate the normalization of these data because the convergence of the search was critical and a function of the starting parameters. The best fit was obtained when the three radius parameters were kept fixed to 1.285 F ($N\chi^2=118$). At this stage of the analysis the χ^2 was not improved very much by renormalizing the data (104 rather than 118); however, when all the parameters were fixed to the average geometry the renormalization improved the χ^2 by a factor of 1.7.

B. Discussion of Results

Because ^{54}Fe has a (p,n) threshold above 9 MeV, we expect some strong contamination of compound nucleus contribution. The only nucleus for which the total search shows very different results from the average is ^{48}Ti.

TABLE II. Justification of the elastic cross-section-data normalization factors K adopted during the total searches and used in Tables I and IV.

Element	K	χ_σ^2	χ_P^2	$N\chi^2$
^{59}Co	1.00	2.4	0.78	87
	0.90	1.1	0.88	48
^{62}Ni	1.00	0.85	0.66	35
	0.95	0.40	0.67	22
^{64}Zn	1.00	1.2	3.2	83
	0.90	0.3	3.6	65
^{66}Zn	1.00	1.4	1.5	66
	0.95	0.8	1.5	48

1. Radius parameters. Only four out of the 42 radius parameters are less than 1.20 F and only eight are smaller than 1.25 F. This result is quite different from the higher-energy analyses which gave, for both the real and spin-orbit potential radius parameters, less than 1.20 F.

There is a tendency for the imaginary potential radius parameter to be larger than the real potential radius parameter. However, for only six out of 14 nuclei is the difference larger than 0.03 F.

There is no tendency for the spin-orbit potential radius parameter to be smaller than the real potential radius since this occurs for only six out of 14 nuclei.

For six nuclei (^{52}Cr,^{56}Fe,^{59}Co ^{60}Ni,^{64}Ni, and ^{63}Cu) the difference between the three radius parameters is less than 0.05 F.

2. Diffuseness parameters. For the imaginary and spin-orbit potentials, the diffusenesses are, with only one exception, smaller than the real potential diffuseness. The spin-orbit and imaginary diffusenesses are approximately the same.

V. SEARCH FOR AVERAGE GEOMETRICAL PARAMETERS

In this section the various steps to determine an average set of geometrical parameters are presented. Because of the high (p,n) threshold for ^{54}Fe and because of the very different parameters found for ^{48}Ti, we decided to exclude them from consideration for the determination of a set of average geometrical parameters. The study proceeded in four steps which will now be described.

Step I_1. Analysis for $r_s=r_D=r_{s0}$. As noted previously for six nuclei (^{52}Cr, ^{56}Fe, ^{59}Co, ^{60}Ni, ^{64}Ni, and ^{63}Cu) the

TABLE III. Variation of the total χ^2's when the geometrical parameters of the optical-model potential were gradually restricted to the average values F given in Table IX. The optical-model parameters corresponding to the column T are given in Table I. The well depths corresponding to the column F are given in Table IV. The symbol "<" indicates a ratio of two consecutive $N\chi^2$'s larger than 1.3 but smaller than 2; "≪" indicates a ratio larger than 2. The elastic cross-section data are normalized by the factors K.

			$N\chi^2$				
Element	K	T	I_1	I_2	I_3	I_4	F
^{51}V	1.00	61	68	83	84	92	101
^{52}Cr	1.00	59	60	62	68	91	102
^{56}Fe	1.00	94	96	103	118	118	121
^{59}Co	0.9	48	50	<85	85	87	93
^{60}Ni	1.00	10	13	<23	≪96	98	101
	1.05[a]	8.9	12	≪24	≪53	53	55
^{62}Ni	0.95	22	<34	38	<54	<79	73
^{64}Ni	1.00	146	150	138	141	153	160
^{63}Cu	1.00	38	≪96	101	<154	154	161
	0.95[a]	28	≪72	80			92
^{65}Cu	0.90	104	105	120	127	127	141
^{64}Zn	0.90	65	<86	91	117	127	125
^{66}Zn	0.95	48	59	55	57	57	62
^{68}Zn	1.00	23	<33	34	42	44	≪84

[a] Renormalization performed only after the geometrical parameters have been fixed to the average values in F.

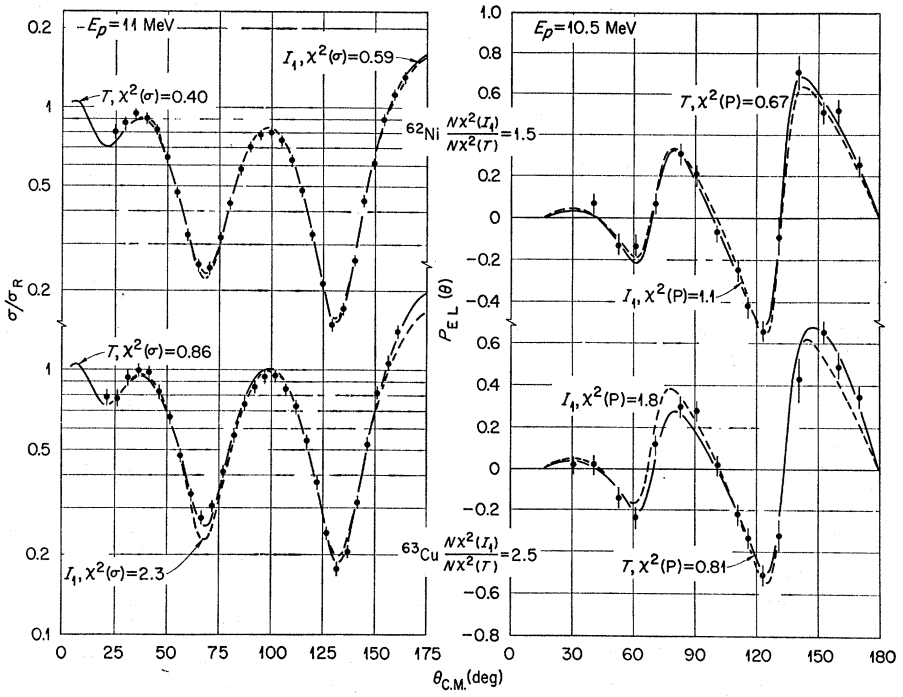

FIG. 4. Examples of worsening of fit quality as a function of the χ^2's ratio. The full curves are the fits obtained to the data when all the parameters were free (search labelled T in Table III); the dashed curves are the fits when the only constraint was to have the three radius parameters to be equal for each nucleus (search labelled I_1 in Table III).

difference between the three radius parameters was less than 0.05 F. This fact led us to reanalyze the data with the constraint that all three radii be the same for a given nucleus. We shall call I_1 those results. The radius parameters so obtained for all 12 nuclei are shown in Fig. 3 and the X^2 are in Table III, where they can be compared to the result of the searches without any constraint on the parameters (labelled Search T).

We rely very heavily, as an objective criteria, on the value of χ^2 to judge the quality of a fit. However, as a practical matter it is often difficult to judge subjectively which of two fits is better when their χ^2's differ only by a ratio of 1.3. We shall therefore refer to two fits as being equivalent when the ratio of their χ^2's is less than 1.3. In Table III we have indicated by the symbol "$<$" when this ratio is greater than 1.3 and by "$\ll$" when it is greater than 2. To demonstrate this point we have shown in Fig. 4 the fits for the two nuclei, ^{62}Ni and ^{63}Cu, for which the χ^2's got the highest increase from T to I_1. Only in the case of ^{63}Cu is the fit noticeably worse. This is not surprising since inspection of Table I shows that it is the nucleus for which there is the greatest difference in radius parameters. For the polarization in Fig. 4, the two sets of curves are somewhat different but give equivalent fits out to 140°.

The average value of the radius parameters is 1.285 F and, with the exception of ^{59}Co, they all lie within $\pm$0.025 F of this value. We note that with this constraint the radius parameter found here is higher than 1.25 F, the value used in several previous analyses near our energy.

Step I_2. Analysis for $r_s=r_D=r_{s0}=1.285F$. The next phase consisted of fixing the average radius parameter at 1.285 F for all nuclei and readjusting all of the other parameters for a best fit. The results of this procedure will be called I_2. The χ^2's are shown in Table III. Only ^{59}Co and ^{60}Ni see their χ^2's increase by more than a factor of 1.3. The case of ^{60}Ni is interesting because, as shown in Fig. 3, its radius parameter is not further away from the average than those for ^{51}V, ^{63}Cu, and ^{64}Zn and it illustrates markedly the different sensitivity of similar curves to variations of optical-model parameters.

Figure 5 shows, with open circles, the values of the two real-well parameters V_s and a_s, which were readjusted. The average value of 0.65 F for a_s, which is often used in this energy range,[4] is in good agreement

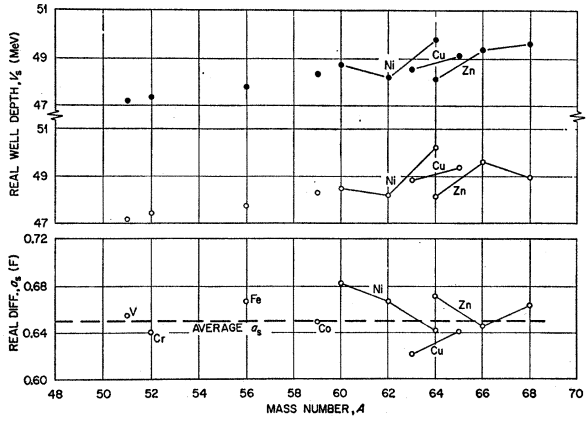

FIG. 5. The open circles are the values of V_s and a_s obtained from search I_2. The radius parameters were set to r=1.285 F and the six other optical-model potential parameters were adjusted by the code to obtain the minimum total χ^2's given in column I_2, Table III. The full circles are the values of V_s obtained from search I_3 with r=1.285 F and a_s equal to the average value of 0.65 F (dashed line).

TABLE IV. Optical-model parameters corresponding to the curves plotted in Figs. 8 and 9. The geometrical parameters were fixed to the average values F given in Table IX. The three well depths were allowed to vary in order to obtain the minimum total χ^2's. The elastic cross-section data are normalized by the factors K.

Element	K	V_s (MeV)	W_D (MeV)	V_{s0} (MeV)	σ_R (mb)	χ_σ^2	χ_P^2	$N\chi^2$
^{48}Ti	1.00	46.52	10.27	8.60	925	12.	20.	693
^{51}V	1.00	47.45	10.41	7.39	941	1.8	3.1	101
^{52}Cr	1.00	47.11	8.96	9.95	882	1.1	4.2	102
^{56}Fe	1.00	47.80	11.27	7.51	934	2.7	2.7	121
^{58}Fe	1.10	48.16	11.51	5.53	962	3.5	4.0	144
^{59}Co	0.90	48.23	11.33	6.84	944	2.2	1.4	93
^{60}Ni	1.05	48.52	10.87	7.85	923	1.2	1.2	55
^{62}Ni	0.95	48.87	11.15	5.62	950	1.5	1.9	73
^{64}Ni[a]	1.00	49.09	11.39	6.11	978	1.4	3.8	160
^{63}Cu	0.95	48.61	10.41	6.38	923	2.5	1.2	92
^{65}Cu	0.90	49.00	10.00	7.56	942	3.0	3.2	141
^{64}Zn	0.90	48.70	10.61	5.76	908	1.9	4.5	125
^{66}Zn	0.95	49.19	10.81	5.84	935	1.2	1.6	62
^{68}Zn	1.00	49.25	11.29	5.17	963	1.5	2.6	84

[a] ^{62}Ni and ^{64}Zn polarization data used.

with those results. The greatest departure from this average value is 0.03 F. We shall, therefore, fix the diffuseness parameter of the real well to 0.65 F.

Step I_3. Analysis for $a_s=0.65$ F. In the following step, called I_3, the three radius parameters are fixed at 1.285 F and the real diffuseness parameter a_s at 0.65 F. All the other parameters are readjusted for a best fit. The χ^2's obtained with those constraints are shown in Table III. The open circles on Fig. 6 show the resulting diffuseness parameters a_D and a_{s0} and the full circles on Fig. 5, the new V_s (very similar to the previous ones).

The average value of a_D is 0.52 F and is shown as a dashed line on Fig. 6. The greatest departures from this average value are +0.095 and −0.075 F. This spread of values is from three to four times larger than that found at the previous step I_2 for a_s.

For the parameter a_{s0} the spread of values is even larger than for a_D. Very often this parameter "runs away" from acceptable values during the automatic search (^{59}Co, ^{62}Ni, ^{64}Ni, ^{63}Cu, and ^{65}Cu) usually in order to improve the fit on the differential cross section at the expense of the fit to the polarization. We had hoped that if we left this parameter free until the end it would assume more reasonable values (did not seem to be true).

Comparing columns I_2 and I_3 in Table III, we see that for three nuclei the values of χ^2's have increased appreciably. We shall now consider each case separately.

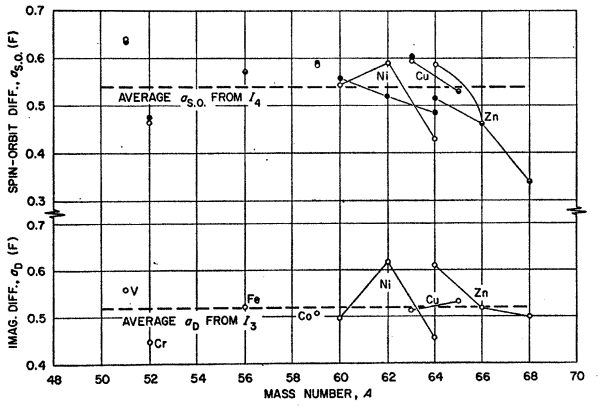

FIG. 6. The open circles are the values of a_D and a_{s0} obtained from search I_3. In this search, $r=1.285$ F, $a_s=0.65$ F, and the five other optical-model potential parameters were adjusted by the code to obtain the minimum total χ^2's given in column I_3, Table III. The full circles are the values of a_{s0} obtained from search I_4 with $r=1.285$ F, $a_s=0.65$ F, and a_D equal to the average value of 0.52 F (dashed line).

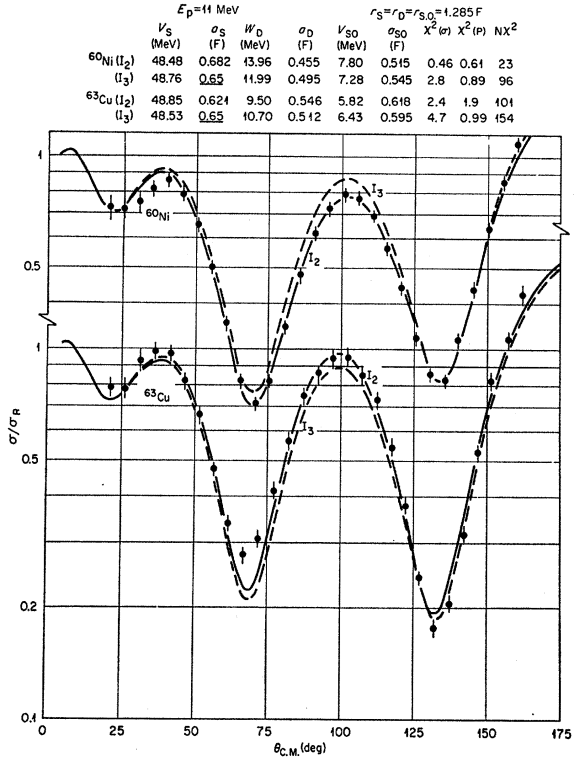

FIG. 7. Comparison for ^{60}Ni and ^{63}Cu of two elastic differential cross-section data fits corresponding to the consecutive searches I_2 and I_3 showing the effect of the variation of a_s.

(a) For ^{62}Ni the total $N\chi^2$ has increased by a factor of 1.4, χ_p^2 has remained unchanged at 1.2 per point, but for χ_σ^2 the value has increased from 0.71 to 1.2 per point. We, therefore, still have acceptable fits.

(b) The differential cross-section fits for ^{60}Ni and ^{63}Cu for both stages I_2 and I_3 are shown in Fig. 7 together with the parameters. For ^{60}Ni changing a_s from 0.682 to 0.65 has caused an increase of 5 to 10% in the calculated differential cross sections for intermediate angles. For ^{63}Cu, changing a_s from 0.621 to 0.65 has decreased the calculated cross sections in the same angular range from 2 to 7%. Fixing a_s at 0.65 F for both

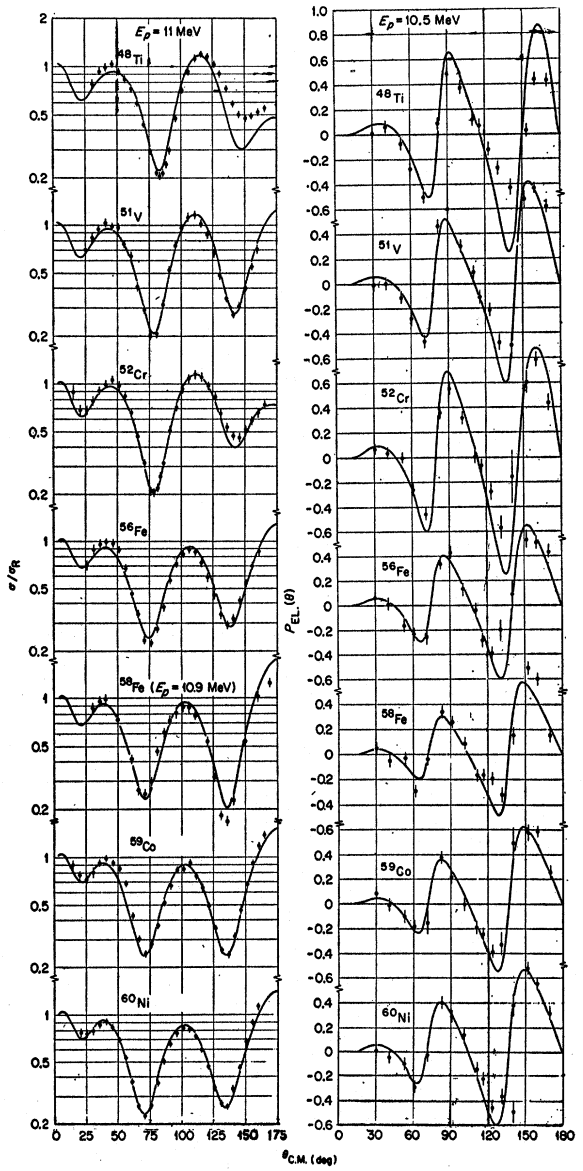

FIG. 8. Fits to the 11-MeV elastic cross-section and 10.5-MeV elastic-polarization data using the average geometrical parameters F, given in Table IX. The three well depths, given in Table IV, were adjusted by the code in order to obtain the minimum total χ^2 for each nucleus.

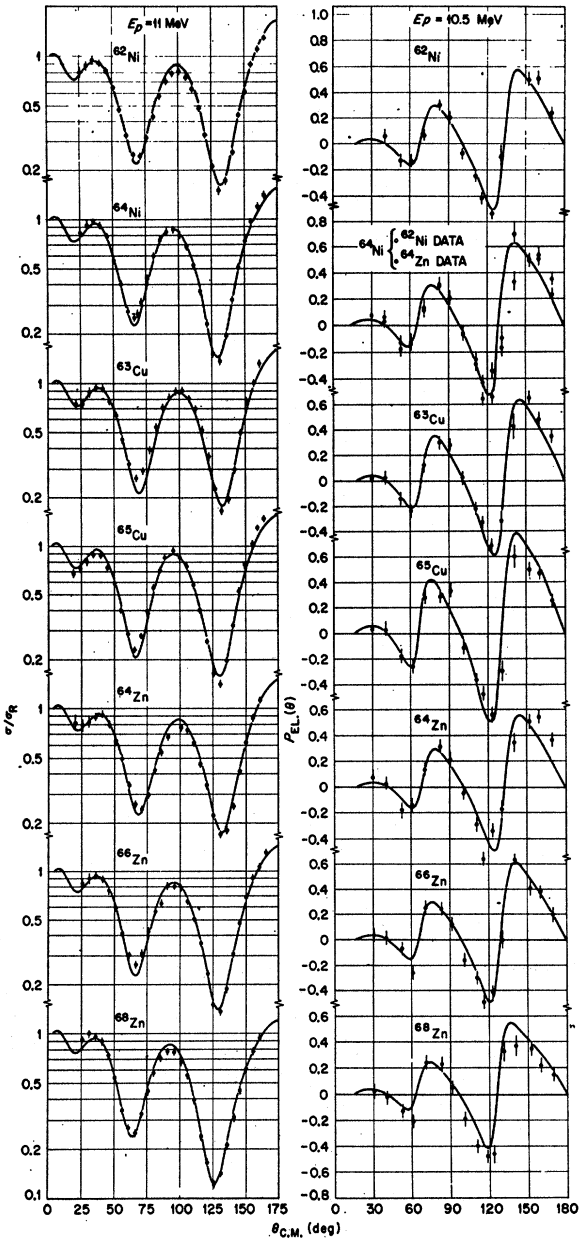

FIG. 9. Fits to the 11-MeV elastic cross-section and 10.5-MeV elastic-polarization data using the average geometrical parameters F, given in Table IX. The three well depths, given in Table IV, were adjusted by the code in order to obtain the minimum total χ^2 for each nucleus.

of those nuclei will be responsible for the renormalization of those data which we will discuss later on.

Step I_4. Analysis for $a_D = 0.52$ F. With the three radius parameters held at 1.285 F, a_s at 0.65 F, and a_D at 0.52 F, the next set of searches labelled I_4 gave fits very similar to those of I_3 as shown by the χ^2's given in Table III even though four nuclei had the value of a_D changed by more than 0.04 F.

The new values of a_{s0} are shown by full circles in Fig. 6. In general the value of a_{s0} is changed very little with

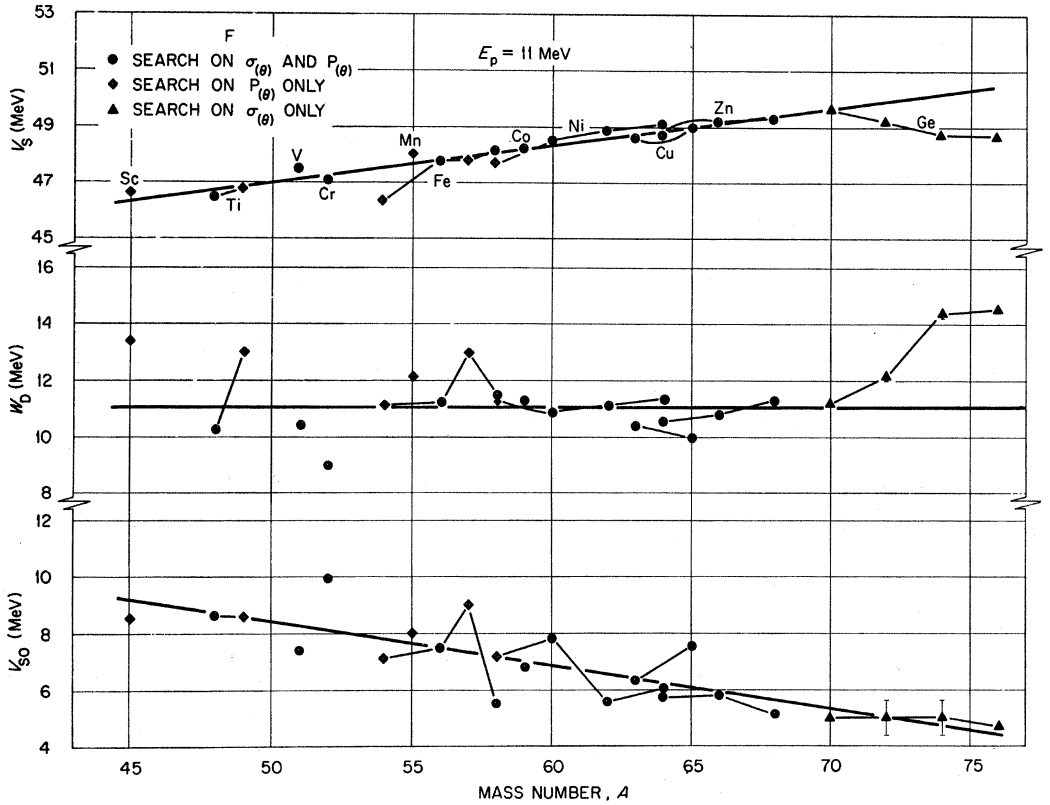

FIG. 10. Well depths as a function of mass number when the geometrical parameters were fixed to the average values F, given in Table IX, and the three well depths adjusted by the code to obtain the minimum total χ^2's. The numerical values are given in Tables IV, VI, and VIII.

the exception of ^{62}Ni, ^{64}Ni, and ^{64}Zn, which had the greatest departure from the average value of a_D, and the new values of a_{s0} followed the same variation as has occurred in a_D. For ^{52}Cr the effect is in the same direction but much smaller. The dashed line at $a_{s0}=0.54$ F is the average value of a_{s0}. The value of 0.339 for ^{68}Zn was not included in this average.

In view of the large spread in the values of a_D and a_{s0} and because their average value differs by only 0.02 F, we decided to set the average value of a_D and a_{s0} to be the same at 0.53 F.

The search for the average geometry is now complete and we have three numbers which characterize it:

$$r_s=r_D=r_{s0}=1.285 \text{ F}, \quad a_s=0.65 \text{ F},$$
$$a_D=a_{s0}=0.53 \text{ F}.$$

We shall, in the remainder of this paper, refer to this geometry as the F geometry.

VI. FITS WITH THE AVERAGE GEOMETRY

The average geometry determined in the previous section will now be used to analyze various data at 11.0 MeV.

1. Analysis using both differential cross-section and polarization data. At 11 MeV, 14 data sets for which we had both differential cross-section and polarization data were fitted using the average geometry by varying only the three well depths to get a best fit. The parameters are given in Table IV and Figs. 8 and 9 show the comparison with the data. The well depths are plotted as a function of mass number, the full circles, in Fig. 10.

Twelve of those 14 nuclei had been used in the determination of the average geometry and the new χ^2's can be compared to those for the very best fit in Table III. Only for ^{68}Zn is the fit considerably worse. This was expected since for this nuclei all the fits required a very small value of a_{s0}. The polarization fit was much affected by the value of $a_{s0}=0.53$ instead of 0.34. The χ_p^2 has gone from 1.1 at I_4 to 2.6 and the χ_σ^2 from 0.95 to 1.5 We note that now the values of χ^2's for this nucleus are comparable to those for other nuclei whereas before these values were much smaller than for other nuclei.

The nucleus ^{48}Ti had been dropped from consideration for the determination of the average geometry because its best-fit parameters were very different from those of the other nuclei. The fit shown in Fig. 8 gives satisfactory agreement out to 125° but the data are much larger than the calculation at back angles and in general the calculated polarization is also larger than the data for those angles. Both of those problems may be caused by the presence of some compound elastic

TABLE V. Justification of the elastic cross-section-data normalization factors K, used in Table IV, adopted during the searches performed with the average geometry F given in Table IX.

Element	K	χ_σ^2	χ_P^2	$N\chi^2$
^{58}Fe	1.00	6.6	4.6	225
	1.10	3.5	4.0	144
^{60}Ni	1.00	2.8	1.2	101
	1.05	1.2	1.2	55
^{63}Cu	1.00	4.9	1.1	161
	0.95	2.5	1.2	92

scattering. However, this cannot be the whole explanation because the amount of compound elastic scattering should be related to the value of the (p,n) threshold, and ^{52}Cr, ^{56}Fe, ^{60}Ni, ^{64}Zn, and ^{66}Zn have (p,n) thresholds higher than ^{48}Ti and their fits do not present the same problem.

In the case of ^{54}Fe compound elastic scattering is certainly important since the ^{54}Fe (p,n) threshold is above 9 MeV; furthermore, we have not succeeded in obtaining satisfactory fits with the average geometry.

At this stage of the analysis we reconsidered the normalization of three angular distributions. Table V gives the comparison of the χ^2 values before and after normalization. For ^{60}Ni and ^{63}Cu renormalization became necessary when the real potential diffuseness was fixed at 0.65 F as shown in Fig. 7 and discussed previously. We reinvestigated the total searches for ^{60}Ni and ^{63}Cu with the new normalization and the results are shown in Table I. Since the parameters are very close to those found previously and the values of χ^2's are slightly smaller than before we felt there was no inconsistency. The slight improvement in χ^2 would not have passed our criteria for renormalization on the basis of the total search results only.

2. Fits to the germanium differential cross-section data. At the time this analysis was performed preliminary differential cross-section data for the four even-even isotopes of germanium had been obtained. To extend the analysis to larger A value, we decided to include those data even though they are poorer than data for the other nuclei, in particular with respect to normalition, and there are no polarization data available.

TABLE VI. Optical-model parameters corresponding to the curves plotted on Fig. 11. The geometrical parameters were fixed to the average values F given in Table XI. The real and imaginary well depths were allowed to vary in order to obtain the best fits to the elastic cross-section data (no elastic-polarization data available).

Element	K	V_s (MeV)	W_D (MeV)	V_{s0} (MeV)	σ_R (mb)	χ_σ^2
^{70}Ge	0.90	49.62	11.21	5.00[a]	930	1.5
^{72}Ge	0.90	49.21	12.15	5.00[a]	958	0.65
^{74}Ge	0.95	48.70	14.35	5.00[a]	989	1.6
^{76}Ge	[b]	48.64	14.52	4.70[a]	1007	1.1

[a] Value of parameter not adjusted by the code.
[b] Data for angles larger than 85° renormalized by 1.2.

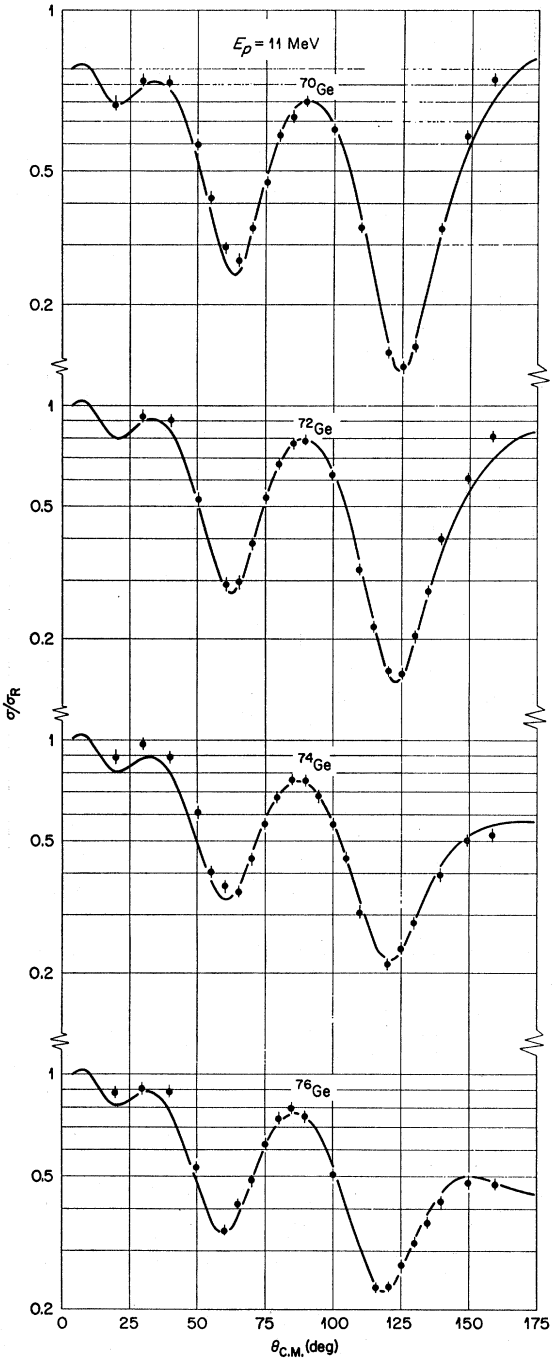

FIG. 11. Fits to the 11-MeV elastic cross-section data of the germanium isotopes when the geometrical parameters were fixed to the average values F, given in Table IX. The three well depths, given in Table VI, were adjusted by the code to obtain the minimum χ_σ^2's.

Since only differential cross-section data were available, we fixed the spin-orbit potential strength to agree with the trends for lighter nuclei. The fits obtained using the average geometry and varying only the real and imaginary potential well depths are shown in Fig. 11. The parameters and the normalization adopted are

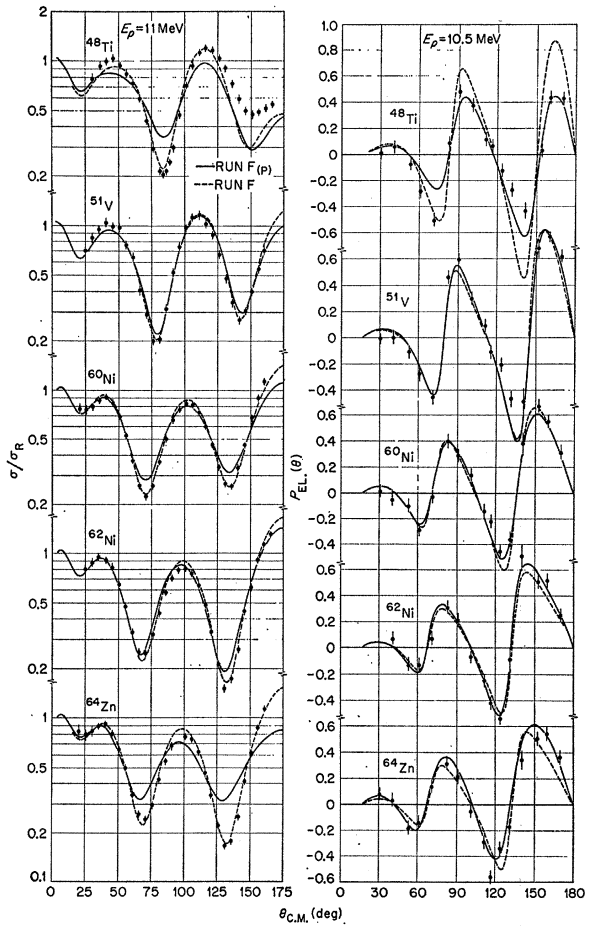

FIG. 12. Comparison with the data of the theoretical curves obtained with the average geometrical parameters F, given in Table IX, when the three well depths were adjusted by the code to obtain the best fits to the elastic cross-section and polarization data simultaneously (dashed curves and Table IV) or to obtain the best fits to the elastic-polarization data only (full curves and Table VII).

given in Table VI and the well depths are plotted as triangles in Fig. 10.

For the two heaviest isotopes ^{74}Ge and ^{76}Ge the real and imaginary well depths seem to depart from the trends of the lighter nuclei when one considers their value as a function of mass number. On ^{72}Ge and ^{74}Ge we varied the spin-oribt potential strength by $\pm 12\%$ but this affected neither the χ^2 values nor the real well depths; the imaginary well depths were affected by only 1 to 2%. The failure of the real and imaginary potentials for ^{74}Ge and ^{76}Ge to follow the trends as a function of A must, therefore, not be associated with the uncertainty in the value of the spin-orbit parameters.

3. Fits using polarization data only. In the mass region where we have analyzed polarization and differential cross-section data, Rosen *et al.* have reported polarization measurements on four odd-mass isotopes, ^{45}Sc, ^{49}Ti, ^{55}Mn, ^{57}Fe, and one even-even isotope, ^{58}Ni, for which we have no differential cross-section data. In the case of ^{58}Ni, we anticipate that we will have a large contribution from compound elastic scattering, as was the case for ^{54}Fe, because of the high (p,n) threshold.

In order to study the relationship between the parameters found by analyzing only polarization data and those where both polarization and differential cross-section data are used, we first analyzed the polarization for five nuclei (^{48}Ti, ^{51}V, ^{60}Ni, ^{62}Ni, and ^{64}Zn) which we had previously analyzed. The parameters are given in Table VII and the comparison with the data shown in Fig. 12 (full curves). Comparing Tables VII and IV, we notice that, although an improvement in χ_p^2 is noticeable (up to a factor of 4.5 for ^{48}Ti and 2.1 for ^{64}Zn), the real-well depths are changed by 0.5 MeV at most, or 1%, but the imaginary potential- and spin-orbit potential well depths have a tendency to be much higher when only the polarization is fitted. For three nuclei (^{48}Ti, ^{60}Ni, and ^{64}Zn) where the increases are the greatest (about 30%), the theoretical curve for the differential cross sections are much more damped than the data. On four cases the differential cross section oscillations are in phase with the data but in the case of ^{64}Zn they are off by about 5°. We, therefore, conclude that the analysis of the polarization data only will most likely yield a real well depth within 0.5 MeV of that which would be obtained if both differential cross-section and polarization data were available but that the imaginary well depths and spin-orbit potential well depths may be too large by up to 30%.

The parameters obtained by fitting the polarization data for the five new nuclei and ^{54}Fe are given in Table VIII and the corresponding curves are shown in Fig. 13. The three well depths are plotted as diamonds in Fig. 10 and the comparison with the other well depths clearly shows the tendencies expected for the real and imaginary potentials. With the exception of ^{54}Fe, which we already knew did not agree with the rest of the data, the values of V_s appear to follow the trends of the other nuclei; four of the six distributions just analyzed show much higher value of W_D than the avergae value of 11 MeV previously found. In the case of the spin-orbit potential, only for ^{57}Fe does the value of V_{so} appear to be high with respect to the other ones.

TABLE VII. Optical-model parameters for run $F_{(P)}$ corresponding to the full curves plotted on Fig. 12. The geometrical parameters were fixed to the average values F given in Table IX and the three well depths were allowed to vary in order to obtain the best fits to the elastic-polarization data only.

Element	V_s (MeV)	W_D (MeV)	V_{so} (MeV)	σ_R (mb)	χ_P^2
^{48}Ti	46.02	13.76	8.07	973	4.3
^{51}V	47.05	10.47	8.02	938	2.8
^{60}Ni	48.15	12.08	9.19	934	0.8
^{62}Ni	49.29	11.71	7.00	962	1.2
^{64}Zn	48.61	13.15	11.14	935	2.1

VII. SYSTEMATICS OF POTENTIAL DEPTHS WITH THE AVERAGE GEOMETRY

1. Variation of parameters as a function of mass number. The values of the parameters for the 24 nuclei analyzed are given in Tables IV, VI, and VIII and are plotted on Fig. 10. To a first approximation we shall consider that the parameters have a linear dependence on the mass number A. Least-square fits to a linear dependence on A were made giving a weight of 2 to the parameters obtained from fits to both differential cross sections and polarization data.

The real well depth V_s is given by

$$V_s = 40.5 + 0.13A \text{ MeV},$$

calculated with 22 nuclei (the results for ^{74}Ge and ^{76}Ge were omitted). If one excepts ^{54}Fe($\Delta V_s = 1.2$ MeV) and ^{72}Ge($\Delta V_s = 0.64$ MeV), all of the other values of V_s are given by the formula to better than 0.4 MeV or 0.8%.

For the imaginary well depths W_D, since there is a considerable scatter of points and no systematic dependence on A, the average value of W_D (excluding again ^{74}Ge and ^{76}Ge) is 11.0_5 MeV. Ten W_D values are within 0.5 MeV of this value and 16 of them within 1 MeV. Seven of the eight points outside of the 1-MeV band are from the analysis of data containing either differential cross sections or polarization data only.

For the spin-orbit potential strength, V_{s0}, the 20 points have a considerable scatter but there is a definite trend for V_{s0} to decrease as a function of A. The least-square fit straight line is

$$V_{s0} = 16.1 - 0.155A \text{ MeV}.$$

Nine of the 20 points are within 0.4 MeV of the line and 16 of them within 1 MeV of it.

2. The isotopic spin dependence of the real potential well depth. It is usually recognized that, at a given bombarding energy, the real part of the effective local potential obtained from proton elastic scattering studies should vary as a function of target nuclei because of (a) the isotopic-spin dependence of the potential and (b) the change in Coulomb potential of the target nuclei.

Since the effective potential is known to be momentum-dependent (the potential decreasing as the momentum increases), the change in momentum due to the increase in Coulomb potential, as we go to larger Z values, will bring about an increase in the effective local potential. It is possible to estimate the magnitude of this effect[4] and many analyses[1–4] consider a contribution of about $0.4Z/A^{1/3}$ MeV to the central real potential due to it.

TABLE VIII. Optical-model parameters corresponding to the curves plotted on Fig. 13. The geometrical parameters were fixed to the average values F given in Table IX and the three well depths were allowed to vary in order to obtain the best fits to the elastic-polarization data (no elastic cross-section data available except for ^{54}Fe but they were not fitted in this search).

Element	V_s (MeV)	W_D (MeV)	V_{s0} (MeV)	σ_R (mb)	χ_P^2
^{45}Sc	46.61	13.38	8.53	963	2.8
^{49}Ti	46.80	12.98	8.59	976	2.8
^{54}Fe	46.36	11.13	7.12	908	2.2
^{55}Mn	47.99	12.16	7.96	961	2.4
^{57}Fe	47.80	12.98	9.02	962	2.3
^{58}Ni	47.68	11.39	7.20	904	3.7

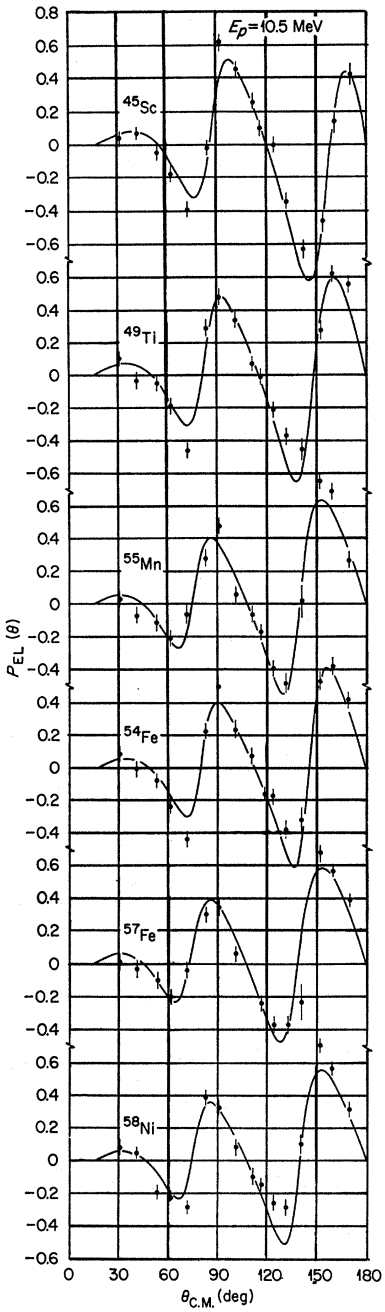

FIG. 13. Fits to the 10.5-MeV elastic-polarization data of six nuclei when the geometrical parameters were fixed to the average values F, given in Table IX. The three well depths, given in Table VIII, were adjusted by the code to obtain the minimum χ_P^2's.

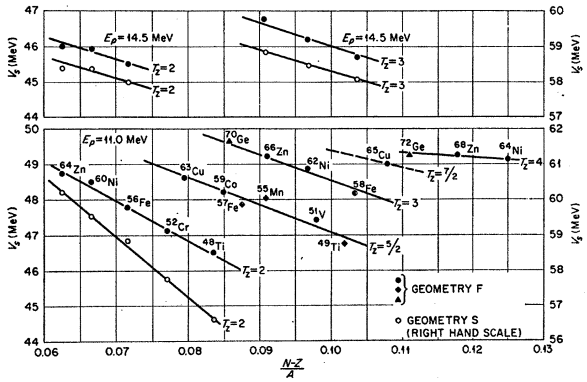

FIG. 14. Real potential well depths V_s as a function of $(N-Z)/A$. At 11 MeV, the full symbols have the same values as those on Fig. 10 obtained with the average geometry F. The open circles are the V_s, given in Table X, obtained with the average geometry S. At 14.5 MeV the plotted V_s are obtained by fitting the elastic cross-section and polarization data of six nuclei with these two sets of average geometrical parameters F and S, given in Table IX.

The isotopic-spin dependence of the optical potential is thought to give rise to a term proportional to $(N-Z)/A$. It is usually assumed that the isotopic-spin term has the same shape as the central real potential, i.e., a Woods-Saxon form. But, in fact, there are some *a priori* reasons for this potential to be peaked near the nuclear surface and some evidence for this in the analysis of charge exchange (p,n) reactions populating the analog ground state.[13] As a practical matter, in optical-model analyses, it is hardly possible to detect whether this term is surface peaked or throughout the volume because of the well-known "VR^n ambiguity." A small change in well depth, if it is a volume term, is equivalent to a small change in radius which would be brought about if the potential was surface-peaked. Therefore, it is not a limitation, in optical-model analyses, to consider the isotopic-spin term to be a volume effect.

If we assume as a first approximation that the Coulomb potentials for the isotopes of an element are the same, then the comparison of the optical potential well depths for different isotopes should yield a value of the isotopic-spin part of the potential free from any correction due to the variation of the momentum inside the nucleus. In our analysis there are six elements for which we have data from two to four isotopes. These are Ti, Fe, Ni, Cu, Zn, and Ge. Because of their (p,n) thresholds, we shall neglect the results for ^{54}Fe and ^{58}Ni. Only for the Ge isotopes do the real well depths fail to increase as a function of mass number as expected. For the other five elements we observe an increase and if within an element we assign this increase to a term proportional to $(N-Z)/A$, its coefficient varies from 10 to 12 MeV. This value is about a factor of 2 smaller than usually found in previous analyses. If all of the real well depths are plotted as a function of $(N-Z)/A$, as shown in Fig. 14, the expected pattern fails to appear. The striking feature of this plot is that the well depths group themselves according to the isotopic spin of the target nucleus. In order to verify that this result is not an artifact of the average geometry chosen, fits were made to all the data for which $T_z=2$ using the very different geometry[8] whose parameters, labelled S, are given in Table IX. The resulting parameters of these fits given in Table X show that, with the exception of ^{48}Ti, the χ^2's obtained are considerably worse than for geometry F, as could be expected, but the new values of V_s still fall on a straight line as shown by the open circles in Fig. 14.

Some 14.5-MeV proton elastic scattering[14] and polarization data[8] were analyzed for nuclei having $T_z=2$ and $T_z=3$ using both the F and S geometries and gave similar results as shown in Fig. 14.

The results shown in Fig. 14 do not necessarily imply a strong T_z dependence of the potential. In fact, they can be shown to be a consequence of the linear dependence of V_s as a function of mass number if one notes that one can write

$$V_s = V_0 + \alpha A = V_0 + 2\alpha \frac{T_z}{(N-Z)/A}$$

and the lines shown are portions of hyperbolas.

3. Comparison with reaction cross sections. All of our analysis has so far ignored the reaction cross-section data which should be reproduced by the optical model. We shall now compare the predictions based on our

TABLE IX. Comparison of our average geometrical parameters F with some others used in previous proton elastic scattering analyses.

	F[a]	R[b]	P[c]	S[d]
r_s(F)	1.285	1.25	1.25	1.12
a_s(F)	0.65	0.65	0.65	0.75
r_D(F)	1.285	1.25	1.25	1.33
a_D(F)	0.53	0.70	0.47	0.58
r_{s0}(F)	1.285	1.25	1.17	1.12
a_{s0}(F)	0.53	0.65	0.47	0.75
r_c(F)	1.25	1.25	1.25	1.20

[a] F: Present work.
[b] R: Rosen *et al.* (Ref. 8).
[c] P: Perey (Ref. 12).
[d] S: Satchler (Ref. 3).

TABLE X. Optical-model parameters obtained from the search code using the geometrical parameters S given in Table IX. The three well depths were allowed to vary in order to obtain the minimum total χ^2's.

Element	K	V_s (MeV)	W_D (MeV)	V_{s0} (MeV)	σ_R (mb)	χ_σ^2	χ_P^2	$N\chi^2$
^{48}Ti	1.00	56.63	9.46	6.25	981	3.5	9.4	257
^{52}Cr	1.00	57.77	8.31	7.79	942	1.8	6.0	156
^{56}Fe	1.00	58.85	9.31	7.19	956	8.3	5.8	326
^{60}Ni	1.05	59.48	9.11	7.95	942	11.	3.5	367
^{64}Zn	0.90	60.15	9.04	6.53	938	8.8	5.2	330

[13] G. R. Satchler, R. M. Drisko, and R. H. Bassel, Phys. Rev. **136**, B637 (1964).

[14] D. A. Lind *et al.* (private communication).

TABLE XI. Comparison of some experimental and calculated reaction cross sections as shown on Fig. 15. The reaction cross sections in column F are calculated with the geometrical parameters F, from Table IX, and the well-depth values from Table IV; in column R are the calculated cross sections from Rosen *et al.*[a]

Element	E_P (MeV)	Calculated σ_R (mb) F	R	Experimental σ_R (mb)
Ti	9.85	889	1007	733±40[b]
	10.2	901	1020	830±44[c]
V	10.0	900	1016	782±62[c]
Fe	9.85	874	969	865±52[b]
	10.2	892	987	759±47[c]
Ni	9.85	841	928	713±40[b]
	10.1	859	948	700±42[c]
^{63}Cu	9.85	848	941	875±61[d]
				845$^{+92}_{-67}$[c]
Cu	10.1	875	964	816±43[c]
^{65}Cu	9.85	867	959	974±76[b]
				855±60[d]
Zn	10.1	873	942	850±43[c]
^{66}Zn	9.85	860	936	946±85[b]

[a] Reference 8.
[b] V. Meyer and N. M. Hintz (Ref. 15).
[c] B. D. Wilkins and G. Igo (Ref. 16).
[d] R. D. Albert and L. F. Hansen (Ref. 17).

analysis with the available data.[15–17] In Table XI two sets of calculations are given, one with the geometry F and the other with geometry labelled R in Table IX. In the case of geometry F the well depths of Table IV for the most abundant isotope were used. The results are plotted in Fig. 15.

The importance of the imaginary potential diffuseness in determining the proton reaction cross section in this energy range has already been pointed out[12] and the geometry F adopted in this work with an a_D of 0.53 F seems to predict too high a reaction cross section by about 50 to 100 mb for the lighter nuclei studied. The geometry R with an a_D of 0.70 F gives a reaction cross section about 100 mb higher than our values and is, in that sense, less satisfactory.

VIII. GLOBAL SEARCH CODE RESULTS

A "global search code"[18] was used to fit simultaneously the data for 11 of the 12 angular distributions previously analyzed for the determination of the average geometry. The code was set up to vary simultaneously the six geometrical parameters of the potentials, but keeping them the same for all 11 angular distributions, and adjust the three well depths independently for each nuclei. The starting values of the parameters for the search code were the geometry F and the well depths given in Table IV. The search converged on the following geometrical parameters:

$$r_s=1.287\text{ F},\quad a_s=0.666\text{ F},$$
$$r_D=1.301\text{ F},\quad a_D=0.512\text{ F},$$
$$r_{s0}=1.274\text{ F},\quad a_{s0}=0.533\text{ F}.$$

The well depths and the χ^2's are given in Table XII. The geometrical parameters are very close to the average geometry F and there is a small improvement in the χ^2's as might be expected since we now have six geometrical parameters rather than three. However, since the parameters are so close to the geometry F and the χ^2's are not changed very much, we conclude that the method used in the search for an average geometry was meaningful and the constraint of setting the three radius parameters equal not very restrictive for the data analyzed.

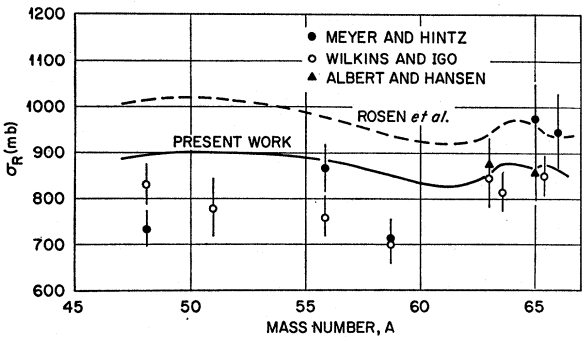

FIG. 15. Comparison of some experimental total reaction cross sections measured around 10 MeV with the calculated ones given in Table XI.

IX. CONCLUSION

One of the purposes of this work was to determine an average optical-model potential for 11-MeV protons elastically scattered from medium-weight nuclei. The search for an average geometry was successful to the extent that the average χ^2 per point (588 data points) for the 12 angular distributions upon which the average geometry was based went from 1.3, with all nine optical-

TABLE XII. Optical-model parameters and χ^2's obtained during the global search. The geometrical parameters were $r_s=1.287$ F, $a_s=0.666$ F, $r_D=1.301$ F, $a_D=0.512$ F, $r_{s0}=1.274$ F, $a_{s0}=0.533$ F. The elastic cross-section data are normalized by the factors K.

Element	K	V_s (MeV)	W_D (MeV)	V_{s0} (MeV)	σ_R (mb)	χ_σ^2	χ_P^2	$N\chi^2$
^{51}V	1.00	47.19	10.96	7.12	956	2.8	3.0	127
^{52}Cr	1.00	46.89	9.46	9.80	900	1.3	4.4	114
^{56}Fe	1.00	47.63	11.82	7.25	947	2.5	2.4	107
^{59}Co	0.90	48.07	11.87	6.73	958	2.1	1.2	83
^{60}Ni	1.05	48.34	11.38	7.72	938	0.63	0.97	34
^{62}Ni	0.95	48.71	11.61	5.70	965	1.1	1.6	54
^{63}Cu	0.90	48.52	10.96	6.18	939	1.6	1.3	68
^{65}Cu	0.90	48.95	10.56	7.25	961	3.0	3.0	138
^{64}Zn	0.90	48.54	11.07	5.88	923	1.1	4.2	98
^{66}Zn	0.95	48.97	11.31	6.00	952	1.5	1.3	66
^{68}Zn	1.00	49.06	11.79	5.40	979	0.84	1.9	55

[15] V. Meyer and N. M. Hintz, Phys. Rev. Letters **5**, 207 (1960).
[16] B. D. Wilkins and G. Igo, Phys. Rev. **129**, 2198 (1963).
[17] R. D. Albert and L. F. Hansen, Phys. Rev. Letters **6**, 13 (1961).
[18] F. G. Perey (unpublished).

model parameters adjusted independently for each nucleus, to 2.2 when the geometrical shape of the potentials for all nuclei was characterized by three numbers and only the three well depths adjusted for a best fit to each nucleus. The optical-model potential geometry we arrived at is different from the ones used at higher proton energies. We did not attempt to obtain a compromise geometry which would be valid at other energies. The geometry we obtained is clearly better suited to the data analyzed since under similar conditions, the geometrical parameters held fixed for all nuclei and the three well depths readjusted for every nuclei, the χ^2's we obtain are more than a factor of 2 smaller than with geometries better suited to the other energies. Because of the longer wavelength and the smaller number of partial waves at 11 MeV the angular distributions are less sensitive to the geometrical parameters than at 30 or 40 MeV. This is reflected by the fact that only three geometrical parameters are required instead of the usual six at higher energies. However, we must emphasize that they are still sensitive enough that the six-parameter geometries used at 30 and 40 MeV give worse agreement with our data than the three-parameter geometry we used.

The major restriction on the geometry was putting the same radius parameters for the real and imaginary potentials. In the five stages of the analysis for the determination of an average geometry the same over-all loss of χ^2 was experienced at each step. This may indicate that the procedure we followed did as much violence to the data at each step including putting the same radius parameter for all potentials. However, this restriction was at the first step when there were still many adjustable parameters; after each step there is one less adjustable parameter. The procedure we followed is very similar to those used at other energies in previous analyses. The global search results are very close to the average geometry and also indicate that the procedure we followed was adequate.

The geometrical parameters found in this analysis are significantly different from those found at higher energies using similar complete sets of data. This is not too surprising since both the shape and the strength of the effective local optical-model potential are expected to vary as a function of energy. Among the factors which will contribute to this energy variation are the effects of exchange terms and the opening of new reaction channels as a function of energy. The major difference in geometrical parameters is the large real potential radius we had to use compared to a value smaller than 1.20 F normally found at higher energies. Since the three radius parameters were set equal it can be argued that the imaginary potential forced a large radius for all the potentials. But inspection of the table of best-fit parameters, when this was not the case, reveals that consistently larger real radius parameters were obtained. Another significant difference in parameters is the smaller value of the imaginary diffuseness parameter. This small value is required for a good fit to both the angular distributions and the reaction cross sections. The value of 0.53 F which we found from the fits to the angular distributions give a slightly too high value for the reaction cross sections at 11 MeV.

Since the effective local optical-model potential should reflect many of the nuclear properties of the target nucleus, it is very surprising that the variation of the real well depth as a function of mass number is so smooth. A linear dependence of the real well depth as a function of mass number predicts the value of the real potential to better than 1%. No effects due to the variation in (p,n) threshold or the different collective properties of the various nuclei are apparent. The behavior of the real well depth when plotted as a function of $(N-Z)/A$ is very puzzling and has been reported and discussed previously.[19] We cannot offer any physical explanation for this dependence which shows too strong a correlation to be accidental. We can rule out our geometry as the cause for this effect since the very different geometry S reproduces it and it cannot be a feature solely of our data since it also appears with the 14.5-MeV data. The pattern in Fig. 14 is due to the fact that we have kept the radius and diffuseness parameters the same for all nuclei and only adjusted the well depths independently for each nuclei. Inasmuch as it is established that small changes in the real radius parameter can be partially compensated by small changes in the real well depth, the correlation observed may be the result both of a systematic change in geometrical parameters as well as in the depth of the potentials. The results of this analysis clearly indicate that at 11 MeV and for medium-weight nuclei, when the radius and diffuseness parameters are kept the same, the effective real potential depths behave in a fashion which is not compatible with only an effective volume isospin potential of the type found in many previous analyses under the same conditions. The imaginary potential well depth shows more fluctuation but no systematic trends can be observed. The spin-orbit potential well depth, even with large fluctuations, shows a systematic decrease as a function of mass number.

X. DISCUSSION

Several attempts[20] have been made at understanding the high-energy optical-model potential in terms of nuclear-matter distribution and the two-nucleon scattering data. Recently the same ideas have been applied to lower-energy nucleon-nucleus scattering.[21–23] Slanina and McManus[22] have shown that, to first order in the

[19] C. M. Perey and F. G. Perey, Phys. Letters **26B**, 123 (1968).
[20] P. E. Hodgson, *The Optical Model of Elastic Scattering* (Oxford University Press, London, 1963).
[21] G. W. Greenlees, G. J. Pyle, and Y. C. Tang, Phys. Rev. Letters **17**, 33 (1966).
[22] D. Slanina and H. McManus, Nucl. Phys. **A116**, 271 (1968).
[23] G. W. Greenlees, G. J. Pyle, and Y. C. Tang, Phys. Rev. **171**, 1115 (1968).

two-nucleon effective interaction, the gross features of the optical-model potential at 30 and 40 MeV could be understood in terms of present knowledge of nuclear density distribution and effective two-nucleon forces. In particular they estimated that the exchange part of the two-nucleon potential was responsible for most of the energy dependence of the optical potential and that at low energy the contribution to the potential due to exchange was appreciable.

From a similar point of view, Greenlees *et al.*[23] have derived the real and spin-orbit parts of the potential, but they neglect entirely the effects of exchange. In their analysis of proton scattering data at 14.5, 30, and 40 MeV, they parameterize the nuclear-matter distribution and the effective nucleon-nucleon potentials, add an imaginary potential, and vary the ten parameters of their model to obtain fits to each angular distribution. In view of the many aspects of the optical-model potential which have been neglected, in particular the effects of exchange and the coupling of other reaction channels, it is not clear that the nuclear density distribution and the effective two-body potentials which they obtain from elastic scattering data fits may have meaning beyond a different parameterization of the real and spin-orbit parts of the optical-model potential, particularly at the lower energies. As a practical matter as many parameters are required in their model as in the conventional approach.

More recently Greenlees *et al.*[24] have disagreed with some of the conclusions of this analysis[19] on the basis of the fits obtained with their model at higher energy.[23] Since we do not concur with them we shall now discuss the two points they have raised. These authors claim that our analysis provides no evidence of any geometrical variation of the potential as a function of energy. This statement is based on the premise that the well-defined geometrical quantity associated with the real central potential is the root-mean-square radius and on the fact that the average geometry we use at 11 MeV gives closely the same root-mean-square radius as the potentials used at 30 and 40 MeV. It has been our experience that if one increases (decreases) the real radius parameter, it is necessary to decrease (increase) the real diffuseness parameter in order to maintain a good fit to the data. As a result the root-mean-square radius changes less than the radius parameter. However, it is not established that elastic scattering is not sensitive to other moments of r. We believe that although the root-mean-square radius of the potential may not change very much, if at all, with energy, it is very significant that the best-fit potentials, and, therefore, the average geometry, at 11 MeV have a greater radius parameter than at 20 and 40 MeV. In fact we find from the work of Greenlees *et al.*[23] some similar evidence when the nuclear-matter distribution, which they obtain at various energies for the same nucleus, has a radius parameter which decreases with increasing energy. The second point which they made is that the variation of V_s with A and $(N-Z)/A$, which we observe, is not meaningful and can be simply interpreted as properties of the particular parameterization chosen. We disagree with this statement which is based on the premise that the well-defined strength information concerning the real central potential is contained in the volume integral of the potential. For a Woods-Saxon potential the volume integral of the potential is given by

$$\tfrac{4}{3}\pi V_s(r_0A^{1/3})^3[1+(\pi a/r_0A^{1/3})^2].$$

Obviously, if r_0 and a are fixed, the volume integral is entirely given by V_s. It is very reasonable to fix r_0 and a, since the data being analyzed have a very fine mesh of A values, and, as pointed out above, the radius and diffuseness we obtained yield a root-mean-square radius consistent with geometries used at 30 and 40 MeV. Fixing r_0, and then determining a from the root-mean-square radius requirement, is, in fact, consistent with the conclusions of their work. Thus, the volume integral of the potential must have the same correlation with $(N-Z)/A$ as that shown in Fig. 14. Furthermore, past experience[25] with optical-model analyses indicates that, for data similar to that analyzed in this paper, the variation of V_s due to uncertainties in the data is $\sim 1\%$. It seems, therefore, that the correlation of V_s with T_z suggested in Fig. 14 is neither fortuitous nor due to some bias introduced by our geometry, but is real and should be studied further.

ACKNOWLEDGMENTS

We would like to thank H. McManus and G. W. Greenlees for communication of their results prior to publication and D. A. Lind *et al.* for sending us their data prior to publication.

[24] G. W. Greenlees, G. J. Pyle, and Y. C. Tang, Phys. Letters **26B**, 658 (1968).

[25] J. K. Dickens, Phys. Rev. **143**, 758 (1966).